

DIMENSIONAL ACCURACY OF SMALL PARTS MANUFACTURED BY MICRO SELECTIVE LASER MELTING

Michael Kniepkamp¹, Jakob Fischer¹, Eberhard Abele¹

¹ Institute of Production Management, Technology, and Machine Tools (PTW), Technische Universität
Darmstadt, Darmstadt, Germany

Abstract

While selective laser melting of metallic parts is already widely used in today's industry, problems in this process still occur when using small parts with dimensions of less than 5 mm. Micro selective laser melting can fill gaps with layer sizes of less than 10 microns and powders with particle sizes smaller than 5 microns. In this paper the dimensional accuracy of parts with sub millimeter features using 316L steel powder is investigated. Test specimens with different features like slopes, overhangs and sharp radii were built applying different scan strategies. The parts were 3D scanned and compared to the CAD data to analyze their accuracy. Based on the results, optimized scan strategies for the different features were developed to increase the parts' overall dimensional accuracy.

1. Introduction

Additive manufacturing (AM) is an emerging field in manufacturing technologies that has the common principle of building up solid parts directly from 3D CAD data by adding material layer by layer. Powder bed fusion based additive manufacturing processes use thermal energy to selectively fuse regions of a powder bed (ASTM F2792-12a 2012). Laser beam melting is a process where powder is applied in layers and then selectively melted using a laser beam to generate three-dimensional parts directly from CAD data. This study focuses on laser beam melting of metal powders, often termed Selective Laser Melting (SLM). Selective laser melting is typically involves layer thicknesses between 20 and 100 μm , using powders with particle sizes ranging from 20 to 45 μm (Gu *et al* 2012). The minimal layer thickness depends on the particle size distribution of the used powder. To increase the resolution and accuracy of selective laser melting, the process has been improved to realize the use of powders with smaller particle sizes enabling layer thicknesses of less than 20 μm (Streek *et al* 2014). Powders with mean particle diameters of less than 10 μm tend to agglomerate, which results in requiring new powder rake systems to process these materials. Since this process differs greatly from the already established SLM process in this study, the term Micro Selective Laser Melting (μSLM) is used. Dimensional accuracy in additive manufacturing describes the geometrical difference between the virtual designed CAD part and the physical part after the build process. Due to the layering manufacturing method, several effects have an influence on the dimensional accuracy of the parts. The machine accuracy describes the mechanical accuracy of the build system, like focused laser spot size, layer thickness and position accuracy of the scanner. The surface morphology, which can be characterized by several effects, also has an influence on the dimensional accuracy. These effects are highly dependent on the relative orientation of the part to the build direction (Strano *et al* 2013). On top facing surfaces, the morphology is dominated by the stability of a single melt track and the hatch distance between two adjacent tracks (Yadroitsev and Smurov 2011, Pupo *et al* 2014). As the top layer is always accessible by the laser, re-melting strategies can be applied to reduce the surface roughness during the build process (Yasa and Kruth 2011). The morphology of side facing surfaces, which are parallel to the build direction, is dominated by partial melted powder particles. Side facing surfaces are surrounded by loose powder particles during the build process. These particles get drawn into the melt pool but due to insufficient energy on the melt pool edge only partial melting occurs. This effect can be influenced by the process parameters laser energy and scan speed (Mumtaz and Hopkinson 2009). The third effect on dimensional accuracy is the distortion of the parts caused by anisotropy and residual stresses. These occur due to high temperature gradients as a result of the locally concentrated energy distortion which may occur when removing the part from the substrate on which it is produced (Kruth *et al* 2010). In selective laser melting different exposure steps are being used. A common strategy is to use two exposure

steps; one for the contour of the part, and one for the core (Meiners 1999). The contour scan vector and its width determines the build accuracy. An beam offset between the parts contour and the contour vector is used to compensate the width of the contour track (Abele *et al* 2015). Benchmark parts are commonly used to measure the machine and process accuracy. Benchmark parts usually have different features, such as slopes, thin walls, overhangs and sharp corners (Byun and Lee 2003, Mahesh *et al* 2004, Kruth *et al* 2005). These parts have been designed so that they do not need a large amount of material in order to be built, to not take too long to build and to be easily and quickly measurable by coordinate measuring machines. Due to their size, up to this date benchmarking parts have not been possible to use for the μ SLM process. In this study, the dimensional accuracy of the μ SLM process is measured using a new test specimen with a maximal diameter of 5 mm based on the typical size of real parts for μ SLM.

2. Research methodology

A commercially available μ SLM system EOSINT μ 60 from the 3D-Microprint GmbH (Germany) was used to conduct the experiments. This system uses a 50 W single mode fiber laser with a wavelength of 1060 nm focused to a spot size of 30 μ m. The laser can be operated in a pulsed or continuous wave mode. In this study, the laser was operated only in the continuous mode, as the pulsed mode leads to discontinuous melt tracks resulting in a high surface roughness. The build platform of the system has a diameter of 60 mm and is moved by piezo actuators with an accuracy of less than 1 μ m. To apply layer thicknesses of less than 10 μ m powders with respectively small particle, diameters have to be used.

Table 1 Reference exposure parameters

Exposure Step	Operation mode	Laser power	Scan speed	Beam offset
1. Core	continuous wave	40 W	1000 mm/s	58 μ m
2. Contour	continuous wave	40 W	500 mm/s	26 μ m

These powders tend to agglomerate. This makes it impossible to coat the powders using gravitational forces only. Thus powder application is achieved by pressing and wiping the powder onto the build platform using external force. The powder used is a 316l gas atomized stainless steel powder with $D_{50} = 3.62 \mu\text{m}$ and $D_{90} = 5.69 \mu\text{m}$. Previous studies using the μ SLM system optimized the build strategy to high relative densities of more than 99 % (Fischer *et al* 2014) and low surface roughness. The result of this is a two-step exposure strategy for the part core and the part contour (Table 1). The parameter setup has a mean roughness R_a on vertical surfaces of 1.69 μm (Abele and Kniepkamp 2015) and less than 1 μm on top surfaces.

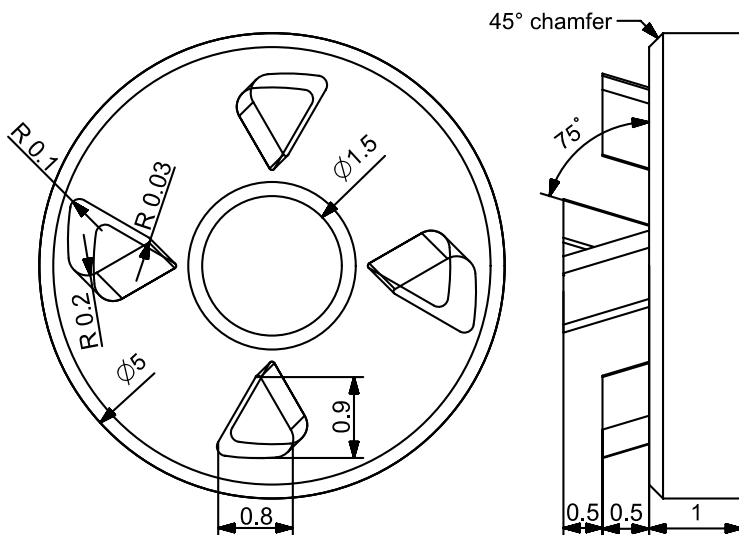


Figure 1 Test specimen to analyze dimensional accuracy (Units: mm)

To analyze the dimensional accuracy of the μ SLM machine, a test specimen based on a typical use case for this process has been used (Figure 1). The part has a tube shaped base plate with an outer diameter of 5 mm and a height of 1 mm. 4 angled pins with heights of 0.5 and 1 mm are on the top. The baseplate is used to analyze larger volumes, outer (5 mm) and inner (1.5 mm) diameters and 45° slopes. The pins are used to measure the accuracy in Z-direction, smaller volumes, small radii (0.1 mm, 0.2 mm and 0.03 mm) and 75° overhangs. To analyze the dimensional accuracy, the specimens were separated from the build platform and three dimensionally scanned using an Alicona InfiniteFocus optical measurement system with an objective magnification factor of 5. Focus variation with a resolution of 410 nm and a rotational unit is used to get a full 360° scan of the test specimens. The software GOM Inspect is used to compare the scanned 3D model with the original CAD designed STEP file. Within GOM Inspect the overall surface deviation and discrete points along critical features of the test specimen are analyzed (Figure 2).

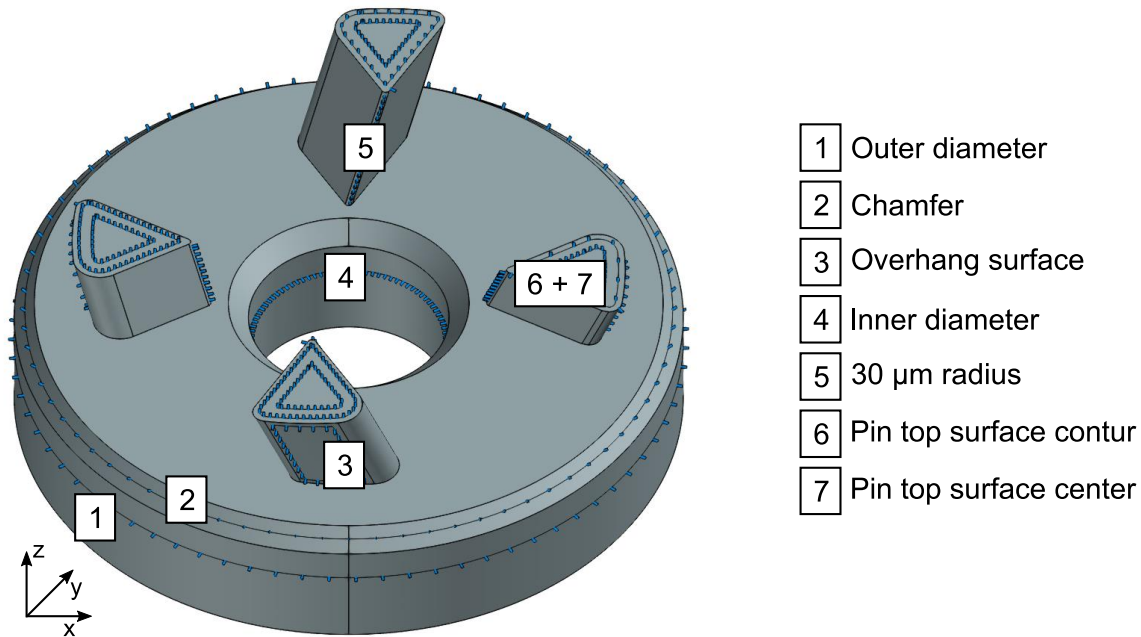


Figure 2 Critical features on the test specimen surface

To determine the reproducibility of the μ SLM system and the dimensional accuracy of the initial exposure strategy (Table 1), 10 specimens were built in two operations, both with an even distribution of the parts across the build platform. To further increase the dimensional accuracy of the initial exposure strategy, further experiments with different strategies were carried out. To increase the accuracy of the pins and the overhangs, the laser power has been reduced to decrease the energy and achieve smaller melt pools. The energy required to generate parts in selective laser melting can be described with the volume energy (E_V) (Meiners 1999), with the laser power (P) the scan speed (v) the hatch distance (h) and the layer thickness (d).

$$E_V = \frac{P}{v h d} \quad (1)$$

The laser power was reduced in 5 W steps to the lower end of the stable line energy of the process window for this material. The hatch distance and the layer thickness were kept constant at 33 μ m and 7 μ m using a scan speed of 1000 mm/s. The resulting volume energies for can be seen in Table 2.

Table 2 Volume energies at reduced laser power

Laser power [W]	40	35	30	25	20
Volume energy [J/mm ³]	173.16	151.52	129.87	108.23	86.58

With a decrease in volume energy, an increase of porosity within the parts is to be expected. To analyze the porosity cubes with lateral lengths of 5 mm have been built using the lowest and the highest volume energies of 173.16 and 86.58 J/mm³. The density was determined using the Archimedes weighting. A downskin build strategy was used to increase the accuracy of the overhanging regions. Separate exposure strategies for the overhanging structures and the rest of the part were used. As the CAM software used for μ SLM does not currently support separate scan strategies for different areas of a part, two parts were generated; one for the overhanging structure, and one for the rest of the part (Figure 3). The width of the downskin structure was set to 0.1 mm and the top layer was excluded from the overhang part. To increase the accuracy of the overhanging structure, the volume energy was reduced to 86.58 J/mm³ and the distance to the part contour was compensated by 19 μ m which is the mean deviation of the reference parameter set. Each specimen was built 5 times and evenly distributed on the build platform.

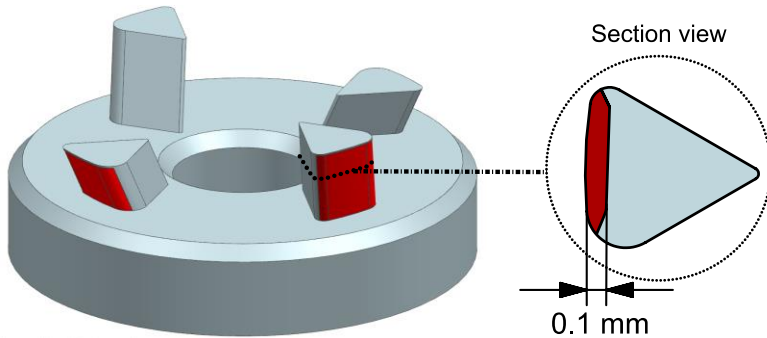


Figure 3 Specimen for overhanging structures. Overhanging structure (red)

3. Results

The results of the dimensional accuracy of the reference parameter setup are summarized in Figure 4. The mean deviation of the inner and outer diameters of the baseplate is within a range of ± 6 microns. In comparison to these results, the deviations of the two chamfers were found to be high with a mean deviation of -17.8 microns and peaks of more than 40 μ m. The two larger radii (0.2 mm and 0.1 mm) of the pins and the sloped surface had low deviations the overhanging surface and the small radius show high deviations of 19.6 and -26.4 microns. The highest deviations from the designed CAD part can be seen on the top surface of the pins. The pin top contour had peak deviations of more than 60 microns in both directions and the mean deviation of the center surface is 13.6 microns higher than designed. The standard deviation of the analyzed features occurred in the layer thickness of 7 microns. However, the pin contour and the overhanging surface had a standard deviation of more than 20 microns.

Feature	Mean deviation [μ m]	Std. dev. [μ m]
Inner diameter	5.4	3.6
Outer diameter	- 4.1	5.7
Pin contour	- 8.2	20.5
Pin center	13.6	6.8
30 μ m radius	- 26.4	6.6
Chamfer	- 17.8	6.7
Overhang	19.6	20.6

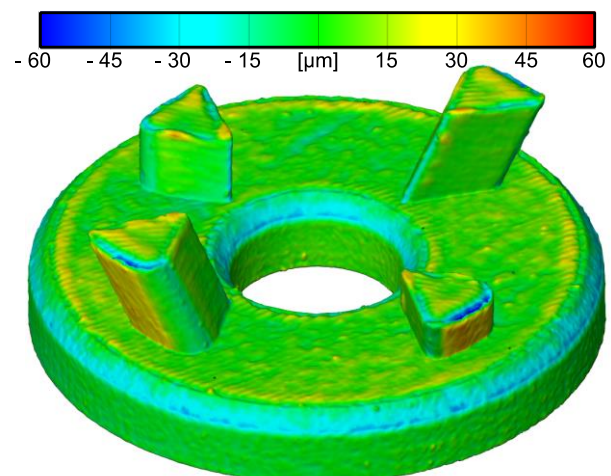


Figure 4 Dimensional accuracy of the reference parameter setup. Mean deviation of the features (left) example of overall surface deviation (right).

The results of the volume energy variation are summarized in Figure 5. Lower volume energies of the parts' core exposure have no significant influence on the outer and inner diameters of the base plate or the 30 microns radius and the overhanging surface. The dimensional accuracy of the chamfers and the top center surface of the pins is increased significantly.

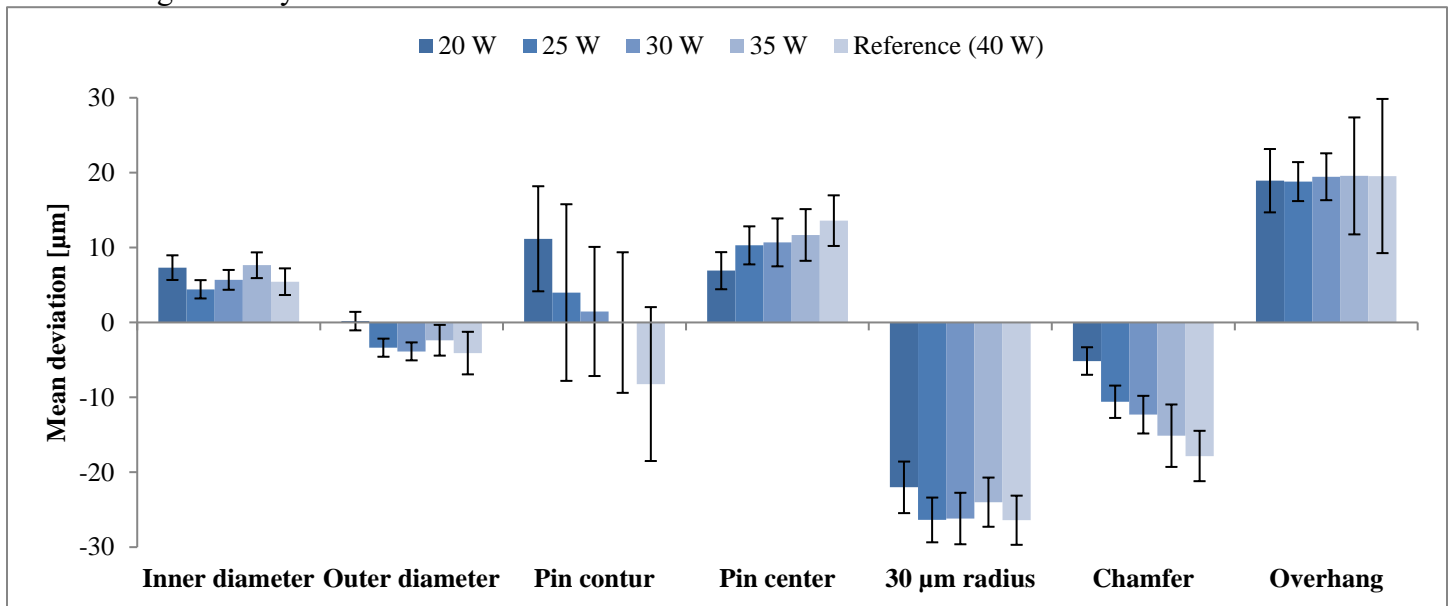


Figure 5 deviations with decreasing volume energies

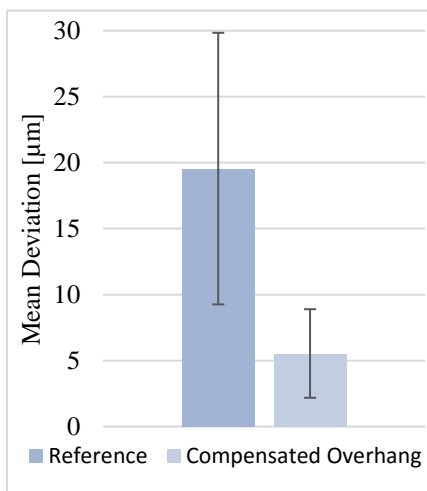


Figure 6 Overhang deviation of the downskin build strategy

Using a volume energy of 86.58 J/mm^3 , the mean deviation of the chamfer can be reduced from -17.8 down to -5.1 microns and on the pin center from 13.6 to 6.9 microns. The mean deviation of the pin contour shifts from -8.2 to 11.1 microns. The standard deviation of the pin contour is between 14 and 20 microns across all laser powers. The density of the high volume energy (173.16 J/mm^3) is at 7.9 g/cm^3 and 7.7 g/cm^3 for the low volume energy (86.58 J/mm^3). The relative density decreased to 97% compared to the reference parameter set (100%).

The deviation of the overhang surface using the downskin build strategy can be seen in Figure 6. The mean deviation in the overhanging structure is reduced from 19.5 microns to 5.5 microns. While the deviation on the flat overhang structure reduced the deviation, the partly overhanging curved surfaces adjacent to it, there was a deviation increase of up to -43 microns.

4. Discussion

To increase the resolution of the selective laser melting process, new machines with higher precision are needed. In theory, reducing the layer thickness and focus diameter should enable generation of smaller parts with a high accuracy. The reference parameter set for the μSLM system was previously optimized towards high densities and low surface roughness. In this study, firstly dimensional accuracy of small parts with dimensions of less than 5mm was investigated. Using the reference parameter setup some areas of the test specimen, such as the base plate, can be built with an accuracy of ± 10 microns. The mean surface roughness for the reference parameter set is lower than 2 microns on the top and side facing sides. In theory, the best possible dimensional build accuracy is within the surface roughness. In reality, other effects also have an impact on the accuracy of additive manufacturing processes. Melt pool dynamics, surface orientation, the coating process and the parts geometry also have an influence on the overall dimensional accuracy. The smallest feature on the test specimen, with a radius of 30 microns, deviate greatly to the designed CAD part. The width of the reference parameters contour

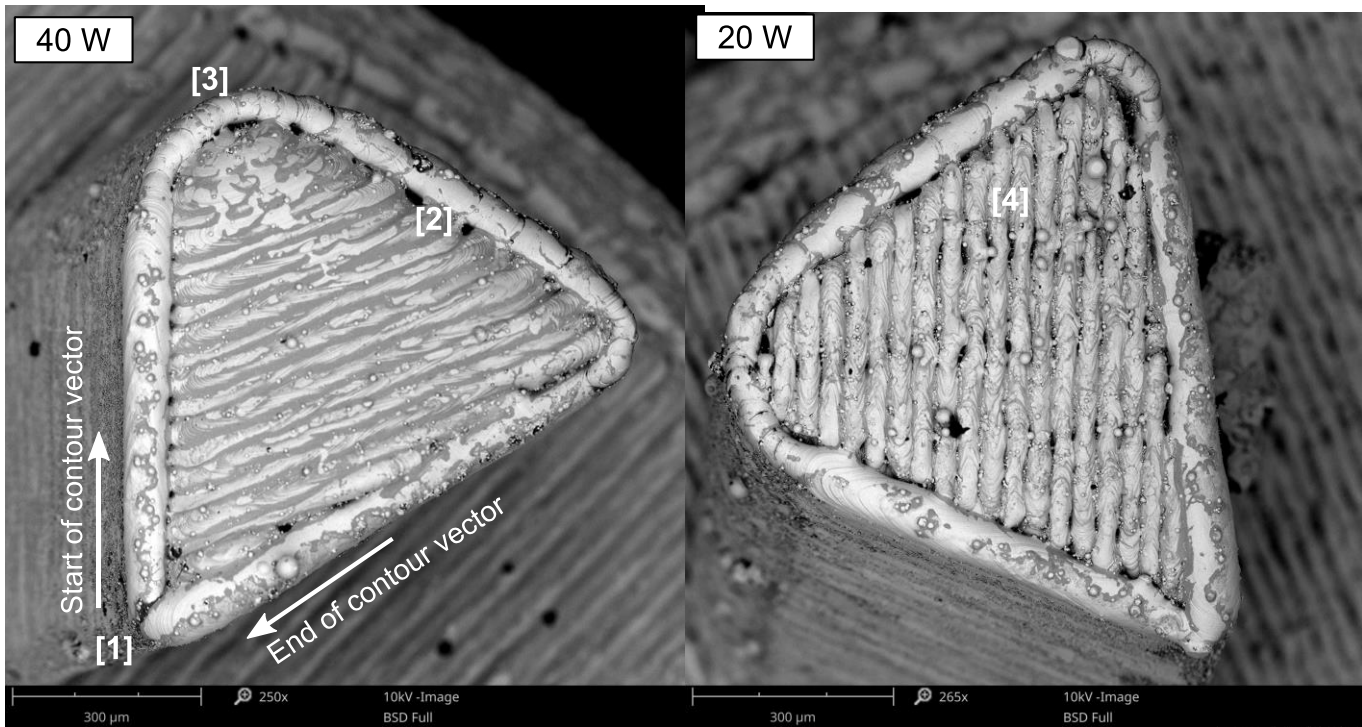


Figure 7 SEM images of the top pin surface with 40 W (left) and 20 W (right) core laser power.

scan track is 52 microns. To compensate the scan track width, a beam offset of 26 microns is used. In theory, the smallest possible radius using this compensation is also 26 microns which is lower than the designed 30 microns of the test specimen. The reason for the negative deviation of the small radius can be explained with the SEM images of the pins top surface (Figure 7). The used CAM software sets the starting and end points of the contour vector on the small radius of every layer [1]. The disconnected melt pool on the edge creates defects and, as a result, the part becomes smaller than the designed size.

The deviations on the top pin contours can also be seen in Figure 7. The SEM images reveal two defects in the contour area. The first one is an insufficient connection between the contour and the core vectors [2]. This results in gaps between the two exposure steps. This can be compensated by decreasing the offset between the core and the contour vectors. The second observed phenomenon is an irregular track width of the contour vector [3]. While it is constant on the straight areas of the contour, it is significantly thinner in the curved areas. Due to the use of the STL file format, the curved areas of a part are triangulated to smaller straight lines instead of a continuous curve. The laser scanner has to rapidly change direction when scanning those smaller lines. This leads to smaller melt pools and results in a thinner track width with a decreasing curve radius.

The variation of the part's core volume energy results in an increase of dimensional accuracy on the pin's top surface and the chamfers. The decrease of the laser power, while keeping the hatch distance, results in thinner track width and gaps between the cores scan vectors (Figure 7) [4]. Less material is molten, which reduces the positive deviation from the designed part on smaller cross sections. A disadvantage of this strategy is the reduced density due to pores in the part and a decrease of the top surface roughness.

In theory, heat dissipation on overhanging structures is lower due to the lower thermal conductivity of the loose powder below the overhanging structure. This effect can be compensated by reducing the volume energy (Mertens *et al* 2014). The deviation in the overhanging parts of the pins cannot be reduced with lower volume energies of the core exposure and constant line energies of the part's contour. With an overhanging angle of 75° and a layer thickness of 7 microns, the theoretical horizontal down facing area in each layer is 1.87 microns. With a track width of 52 microns, the contour exposure step dominates the core exposure in the overhanging area. Reducing the laser power of the contour vector could increase the dimensional accuracy in the overhanging structure with the drawback of a higher surface roughness in on the whole part. Using the down-skin exposure strategy the deviation in the overhanging structure could significantly be reduced by adjusting the contour offset. The

disadvantage of this method is that a different offset is needed for each angle. Another challenge is to generate a smooth transition between the overhanging areas and the rest of the part.

5. Summary and outlook

The present work gives a first impression of the dimensional accuracy of small metallic parts built using micro selective laser melting with layer thicknesses of 7 microns. Test specimens with a maximum dimension of 5 mm have been built using different exposure strategies. The specimens were 3D scanned using optical focus variation and compared to the designed geometry. From the results the following conclusions can be drawn:

- Using a reference exposure strategy optimized for density and surface quality, mean deviations from the designed geometry ranging from -26.4 to 20 microns with peaks of ± 60 microns can be seen.
- The built accuracy of larger cross sections is higher than for smaller ones. The highest deviations can be seen on overhanging structures and on the top surface of small cross sections.
- The accuracy of small cross sections can be increased by decreasing the laser power.
- Using different exposure strategies for the overhanging structures and the rest of the part can be used to increase the accuracy of overhanging areas.

To achieve the best build accuracies in all areas of a part, a uniform exposure strategy should not be used. Future research should analyze in detail which geometrical features require special exposure strategies in order to further increase the dimensional accuracy of μ SLM parts. Furthermore, an automated process needs to be developed, in order to assign different exposure strategies to different areas within one part.

Acknowledgments

This work was partially funded by the Federal Ministry of Economic Affairs and Energy through the AiF GmbH (Grant No. KF2012461WO3). The Authors would like to thank for this support.

References

- Abele E and Kniepkamp M 2015 Analysis and optimisation of vertical surface roughness in micro selective laser melting *Surf. Topogr.: Metrol. Prop.* **3** 34007
- Abele E, Stoffregen H A, Kniepkamp M, Lang S and Hampe M 2015 Selective laser melting for manufacturing of thin-walled porous elements *Journal of Materials Processing Technology* **215** 114–22
- ASTM F2792-12a 2012 *Terminology for Additive Manufacturing Technologies* (West Conshohocken, PA)
- Byun H-S and Lee K H 2003 Design of a New Test Part for Benchmarking the Accuracy and Surface Finish of Rapid Prototyping Processes *Proceedings of the 2003 International Conference on Computational Science and Its Applications: Part III (ICCSA '03)* (Berlin, Heidelberg: Springer-Verlag) pp 731–40
- Fischer J, Kniepkamp M and Abele E 2014 Micro Laser Melting: Analysis of Current potentials and Restrictions for the Additive Manufacturing of Micro Structures *25. Solid Freeform Fabrication Symposium (Austin, Texas)* ed D Bourell pp 22–35
- Gu D D, Meiners W, Wissenbach K and Poprawe R 2012 Laser additive manufacturing of metallic components: materials, processes and mechanisms *International Materials Reviews* **57** 133–64
- Kruth J-P, Badrossamay M, Yasa E, Deckers J, Thijs L and van Humbeeck J 2010 Part and material properties in selective laser melting of metals *Proceedings of the 16th International Symposium on Electromachining*

- Kruth J-P, Vandenbroucke B, van Vaerenbergh J and Mercelis P 2005 Benchmarking of Different SLS/SLM Processes as Rapid Manufacturing Techniques *Proceedings of 1st International Conference of Polymers and Moulds Innovations (Gent, Belgium)*
- Mahesh M, Wong Y S, Fuh J and Loh H T 2004 Benchmarking for comparative evaluation of RP systems and processes *Rapid Prototyping Journal* **10** 123–35
- Meiners W 1999 *Direktes selektives Laser-Sintern einkomponentiger metallischer Werkstoffe* (Aachen: Shaker)
- Mertens R, Clijsters S, Kempen K and Kruth J-P 2014 Optimization of scan strategies in Selective Laser Melting of aluminium parts with downfacing areas *J. Manuf. Sci. Eng.*
- Mumtaz K and Hopkinson N 2009 Top surface and side roughness of Inconel 625 parts processed using selective laser melting *Rapid Prototyping Journal* **15** 96–103
- Pupo Y, Sereno L and Ciurana J de 2014 Surface Quality Analysis in Selective Laser Melting with CoCrMo Powders *MSF* **797** 157–62
- Strano G, Hao L, Everson R M and Evans K E 2013 Surface roughness analysis, modelling and prediction in selective laser melting *Journal of Materials Processing Technology* **213** 589–97
- Streek A, Regenfuss P and Exner H 2014 High Resolution Laser Melting with Brilliant Radiation 25. *Solid Freeform Fabrication Symposium (Austin, Texas)* ed D Bourell pp 377–89
- Yadroitsev I and Smurov I 2011 Surface Morphology in Selective Laser Melting of Metal Powders *Physics Procedia* **12** 264–70
- Yasa E and Kruth J-P 2011 Application of laser re-melting on selective laser melting parts *Advances in Production Engineering & Management* ed Miran Brezocnik (Maribor, Slovenia) pp 238–310